IT-CsF1 TAI EVALUATION
MJD 55334-55349 (May 18th - June 2nd 2010)

Introduction

During the period MJD 55334.0-55349.0, INRiM has evaluated the frequency of its Hydrogen Maser IT-HM2 (BIPM code 1401102) using the Cs fountain primary frequency standard IT-CsF1. The evaluation procedure of the fountain standard follows the general procedures reported in [1, 2]; we report here details on the Type A and Type B uncertainty evaluation, together with the internal transfer uncertainty (including the contribution of dead time).

IT-CsF1 Accuracy Evaluation

Black Body Radiation Shift $\Delta\nu_{BBR}$

The evaluation of the Blackbody Radiation (BBR) Shift $\Delta\nu_{BBR}$ requires to know the effective BBR temperature T experienced by the atoms along their ballistic flight. For the calculation of T, we interpolate the temperature data coming from four thermocouples positioned along the drift tube with a polygonal curve and then we calculate the average radiation temperature experimented by the atoms at a given position (integrated over the solid angle); in this way it is possible to take into account also the effect of the two "holes" in the blackbody radiator, the upper window and the hole in the microwave cavity. The values obtained at different elevations inside the fountain drift tube are then used to calculate the time averaged radiation temperature seen by the atoms along their ballistic flight. See the discussion reported in [3] for details.
To evaluate $\Delta\nu_{BBR}$ from the effective temperature T we follow the well known relation discussed for example in [3] and reported here below; the leading coefficient β here used is calculated using results presented in [4]; the coefficient ε is taken from [5].

$$\Delta\nu_{BBR} = \beta\,(T/300)^4 \cdot [1+\varepsilon(T/300)^2]$$

$$\beta = (-1.711 \pm 0.003) \cdot 10^{-14}$$

$$\varepsilon = 0.014$$

$$T = 66.2 \pm 1.0\ ^\circ C = 339.4 \pm 1.0\ K$$

$$\Delta\nu_{BBR} = (-28.5 \pm 0.3) \cdot 10^{-15}$$

Gravitational Red Shift $\Delta\nu_{RS}$

Gravitational redshift at the IT-CsF1 location was accurately calculated during 2006 and the result from that activity is used here to correct the TAI calibration data. These evaluation data take advantage of some refined gravimetric data, coming from an accurate Geoid regional model and levelling techniques together with precise geometrical measurements of the vertical position of IT-CsF1 with respect to the geodetic reference markers. A detailed description of this work is reported in a Metrologia paper [6].

$$\Delta\nu_{RS} = \gamma \cdot h$$

$$\gamma = 1.09 \cdot 10^{-16}\ m^{-1}$$

$$h = 239.43 \pm 0.03\ m$$

$$\Delta\nu_{RS} = (+26.10 \pm 0.01) \cdot 10^{-15}$$

Quadratic Zeeman Shift $\Delta\nu_Z$

The effective C-field experienced by the atoms (B_0) along their trajectory is calculated (see [1] for details) from a field map which is obtained measuring the low frequency magnetic resonance transitions when the atoms are at the apogee; the map is completed launching the atoms at different apogee heights.

The C-field map is reported in the figure 1 and it was used to calculate the quadratic Zeeman shift by mean of a field integration over the flight time. Reference for the value of the quadratic Zeeman constant K is [7].

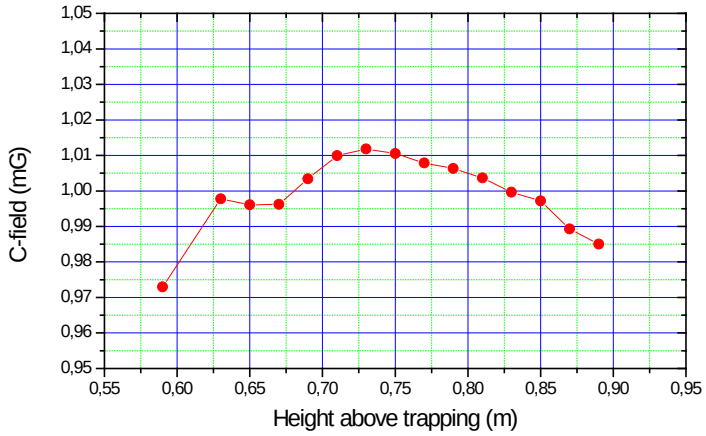

Figure 1. C-field map.

The uncertainty associated to the magnetic field was derived with three independent methods.

First, we evaluated the frequency instability of the clock locked on the central fringe of the magnetic sensitive transition F=3, m_F=-1→ F=4, m_F=-1. This yields to a value that is better than $5 \cdot 10^{-12}$ over one day of measurement. Consequently the instability on the clock transition is $< 1 \cdot 10^{-17}$

Second, the long term instability of the C-field was evaluated comparing mapping results during last year. These results differ by $2 \cdot 10^{-16}$. Adopting a conservative approach, this value is considered an estimation of the stability of dc quadratic Zeeman shift during this run.

The heater used to frequency tune the Ramsey cavity and to stabilize the drift tube temperature is powered with an audio-frequency generator (70 kHz) to avoid the penetration of the generated magnetic field inside the drift tube.

The heater is operated cw during the whole operation cycle of the fountain, in order to prevent a dynamic end-to-end phase shift [6] caused by a temperature modulation of the cavity synchronous with the Ramsey cycle.

Although shielded by several skin depths, a residual rms magnetic field produced by the audio frequency generator could penetrate inside the drift tube, causing a quadratic Zeeman shift of

the clock transition frequency. A calibration of this effect is performed feeding the part of the heater around the drift tube with a known dc power, while the cavities are kept on resonance by the part of the heater around the cavities only (fed as usual by an ac power at 70 kHz), where the thickness of the copper is larger and the shielding effect is estimated higher by several orders of magnitude.
We measured the magnetic field generated by the dc powered heater coils observing the frequency shift of the $F=3,m_F=-1 \rightarrow F=4,m_F=-1$ transition, then we use this value to evaluate the residual magnetic field due to the ac power. The calibration shows that the Zeeman shift due to the ac powered heater is less than $4\cdot10^{-17}$. The total uncertainty on the Zeeman shift correction is then conservatively stated as $2\cdot10^{-16}$.

$$\Delta\nu_Z = K \cdot B_0^2$$

$K= 427.45\ Hz/T^2$

B_0, C-field as calculated with the map

$$\Delta\nu_Z = (+45.7 \pm 0.2) \cdot 10^{-15}$$

Collisional Shift

The collisional shift is evaluated during the fountain run alternating operation at two different densities, labelled HD (high density) and LD (low density). The average density ratio between HD and LD conditions is about 2.5 and the total accumulated run time at LD is 4 times larger than in HD, as in LD the stability is degraded by the low atom number. The density shift is evaluated using the Bayesian techniques described in [13,14]; in particular the average frequency value y(HM2)- y(IT-CsF1) over the evaluation period is obtained with a Bayesian least-square fit described in detail in [14] and in the section "Evaluation of the average frequency y(HM2)- y(IT-CsF1)" later in this document. This technique assumes that the proportionality between the density and the atomic signal (the parameter which is actually detected) is constant during the whole run. To account for a possible deviation from the proportionality (due the instability of detection efficiency) a Type B uncertainty contribution which value is equal to the 20% of the total average of the density shift during the run is assumed.

During the present evaluation, the average value of the cold collision relative frequency shift and the associated type B uncertainty were:

:

$$\Delta\nu_{Coll} = (-0,5 \pm 0.1) \cdot 10^{-15}$$

Other Shifts

The actual influence of other shifts resulting from several physical and technical effects was carefully investigated during the most recent history of IT-CsF1. The contribution of these shifts is either negligible or not easily modelled and then no correction is applied for. Only an uncertainty contribution is provided for these effects, reflecting the estimation of their maximum values during the fountain operation.
These shifts, either theoretically estimated or measured, are [1,2]

- Resonant light shift
- Distributed cavity shift
- Dynamic end-to-end phase shift [8]
- Cavity pulling

- Relativistic Doppler shift
- Synthesizer and numerical loop errors
- Microwave leakage and power-related shifts

In order to estimate the shift and the uncertainty contributions which shows a dependence with respect to the microwave power, the fountain is operated at odd multiples $(2n+1)\pi/2$ (n=1,2...) of the optimum Rabi pulse area ($2b_0\tau = \pi/2$). One of the nastier and more frequent microwave related shifts is the leakage that can occur during the fountain operation.
As it was recently reported [9], the relation between the microwave field amplitude and the leakage induced shift is not linear and can be dramatically different if the leakage occurs between the two Ramsey interrogations or after the second one, before the detection stage.
For these reasons, leverage tests were designed following the theory reported in [9], and different tests were conducted to estimate the shift due to the leakage during different stages of the fountain cycle. In particular, driving the fountain at high microwave power, it has sometimes shown an evidence of a microwave leakage occurring during the time interval between the second Ramsey pulse and the detection.
In the months before the present evaluation, the IT-CsF1 fountain has undergone different changes in the microwave generation and distribution subsystems. The most important of these changes involves the microwave synthesizer, which now shares the same design IT-CsF2 one. The details of this synthesizer are reported in [14] and in [15].
After these big changes, the tests for the microwave power related shifts have been particularly long and in-depth. These tests were conducted during the three months preceding this evaluation and account for about one month of total accumulated running time. Many different tests were conducted but fountain measurements with $\pi/2$, $3\pi/2$, $5\pi/2$, $7\pi/2$ Rabi pulse areas provide results in agreement with the theory reported in [9], showing a microwave leakage occurring during the time interval between the second Ramsey pulse and the detection as it occurred in the past.
The estimation of the microwave leakage shift provided by the tests described before is $< 0.3 \cdot 10^{-15}$.

Summary of accuracy evaluation

Effect	Shift (10^{-15})	Uncertainty (10^{-15})
2nd order Zeeman Shift	+45.7	0.2
Blackbody Radiation Shift	-28.5	0.3
Gravitational Red Shift	+26.1	0.01
Microwave Leakage Shift	--	0.3
Collisional Shift (Systematic)	-0,5 (*)	0.1
Other shifts	--	0.1
Total	**+43.3**	**0.5**

Table 1. Summary of corrected and uncorrected shifts and uncertainty budget for IT-CsF1, MJD 55334-55349. (*) Average value, not accounted for the total correction reported in the last line.

Evaluation of the average frequency y(HM2)- y(IT-CsF1)

During the reported evaluation period, the H-maser HM2 (BIPM code 1401102) was used as local oscillator.

The average frequency *y(HM2)- y(IT-CsF1)* over the period MJD 55334-55349 was evaluated by the average value of *y(HM3)- y(IT-CsF1)* and the phase comparison *y(HM2)- y(HM3)* during the epoch. The average frequency *y(HM3)- y(IT-CsF1)* over the period MJD 55334-55349 was calculated with a linear fit which exploit techniques from Bayesian statistic. Following the example described in [14] (Section 3.5 and 4), the data taken at different densities and epoch are fitted using a two dimensional linear equation of the following form:

$$y=a+bx+ct$$

which fits the data triplet (y_i, x_i, t_i) where the y_i is the value of the measurement *y(HM3)- y(IT-CsF1)* taken at the epoch t_i and at the density x,. The meaning of the parameter a, which can be regarded as $y(x=0,t=0)$, is the estimation of the average frequency *y(HM3)- y(IT-CsF1)* extrapolated to zero density if the epoch coordinate origin is taken on the centre of the evaluation interval (MJD 55341.5 in this particular case). The parameter b is the collisional coefficient and it is used to calculate the average frequency shift for the Type B density uncertainty evaluation and c is the average maser drift over the evaluation period. As it is described in [14], the Bayesian linear least square algorithm here incorporates the condition $b>0$, which correspond to the theoretical evidence that the fountain frequency decreases when the atomic density increases (negative density shift). This condition holds for the operational conditions of atomic temperature, density and quantum state mixtures of IT-CsF1. In the least squared algorithm, the a-priori condition $b>0$ is taken into account in a Bayesian way. The algorithm could also take into account in a Bayesian way an a-priori value and uncertainty for the maser drift (obtained, for example, from a previous fountain run). In this specific evaluation the a-priori condition for the maser drift has been not used.

Fitting the maser drift over the evaluation epoch was chosen because fountain dead (lost) time is unavoidable during the evaluation period, and the dead time intervals are neither evenly spaced nor symmetric with respect to the centre of the evaluation period. In these conditions, dead time would

have biased an estimation derived by a standard average. Epoch distribution of fountain dead time is reported in Figure 2.

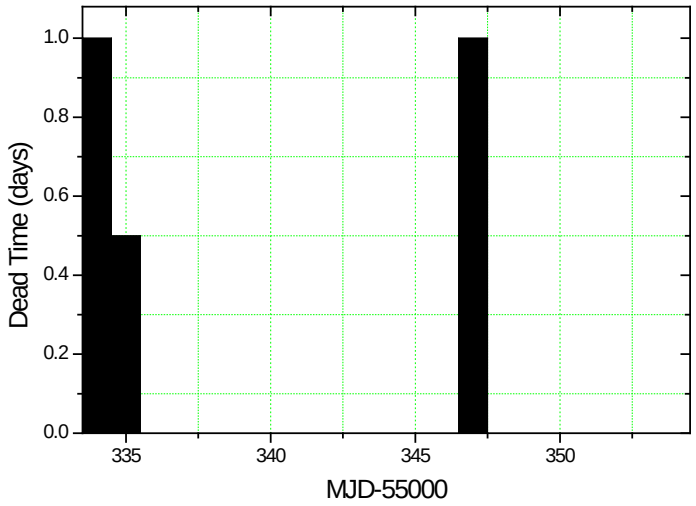

Figure 2. Epoch distribution of the dead time during the present evaluation.

The choice of a linear model for the maser drift takes into account the fact that the HM2 frequency has shown a very stable drift in the past year within periods even larger than 50 days.

The Bayesian linear fit provide an estimation of the uncertainty of the parameters *a ,b, c,* which can be regarded as Type A uncertainty. The uncertainty associated to the average frequency estimation *y(HM3)- y(IT-CsF1)* and reported as Type A, is the uncertainty of the coefficient a as it is estimated by the Bayesian least square algorithm. Figure 3 reports *y(HM3)- y(IT-CsF1)* raw data (red points HD, black points LD, and the Bayesian linear fit curve $y=a+bx+ct$ with $x=0$ (extrapolation to zero density).

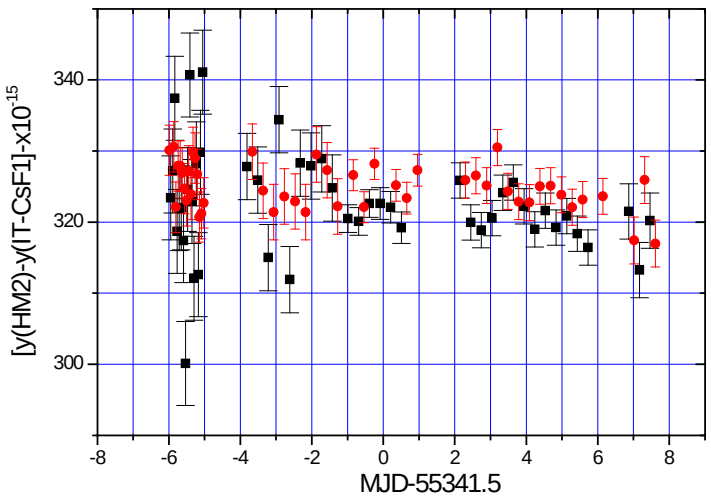

Figure 3. *y(HM3)- y(IT-CsF1)* data and the Bayesian linear fit curve (straight line).

Final results of the statistical analysis is reported in Table 2:

	Value	Uncertainty
HM3 drift (*Coefficient c*)	$-0.35 \cdot 10^{-15}$ /day	$0.08 \cdot 10^{-15}$ /day
y(HM3)- y(IT-CsF1) extrapolated to zero density, MJD 55334-55349 (*Coefficient a*)	$+323.2 \cdot 10^{-15}$	$0.4 \cdot 10^{-15}$
y(HM3)- y(HM2)	$+329.2 \cdot 10^{-15}$	$0.4 \cdot 10^{-15}$
y(HM2)- y(IT-CsF1)	$-6.0 \cdot 10^{-15}$	$0.6 \cdot 10^{-15}$

Table 2. Results of the weighted linear fit $y=a+bx+ct$

Local link and dead time uncertainty (ul/lab)

The HM2 is phase compared to UTC(IT) time scale, which is the reference time scale for remote time and frequency transfer tools, with a Time Interval Counter in the INRiM Time and Frequency laboratory. In this evaluation, we directly evaluated the frequency of the Hydrogen Maser HM3 and than evaluated HM2 frequency using phase comparisons with UTC(IT). This comparisons introduces a uncertainty contribution to the IT-CsF1 transfer to TAI, which is estimated as $0.4 \cdot 10^{-15}$ for this evaluation period (15 days).

Dead time in fountain operation introduces a further uncertainty to the frequency transfer to TAI. The estimation of this uncertainty contribution requires the knowledge of the HM2 noise properties. The stability of HM2 could be modelled in terms of Allan variance, as:

$$\sigma_y^2(\tau) = \sigma_{yWF}^2(\tau) + \sigma_{yFF}^2(\tau) + \sigma_{yRWF}^2(\tau)$$

where $\sigma^2_{yWF}(\tau)$, $\sigma^2_{yFF}(\tau)$ and $\sigma^2_{yRWF}(\tau)$ are respectively the contribution due to white, flicker and random walk frequency noise. A conservative estimation of these contributions is:

$$\sigma_{yWF}(\tau) < 3 \cdot 10^{-13} \tau^{-1/2}$$

$$\sigma_{yFF}(\tau) < 3 \cdot 10^{-16}$$

$$\sigma_{yRWF}(\tau) < 2 \cdot 10^{-19} \tau^{1/2}$$

The dead time uncertainty contribution is calculated with a new and improved technique. Starting from the theory reported in [11], an automated software routine [12], implementing a refined algorithm with respect to [11], can handle the actual dead time distribution of the fountain run and provide an estimation of dead time uncertainty.
The dead time uncertainty contribution, calculated for the distribution shown in Fig 2 using the software routine [12] is reported in the table below

Contribution	Uncertainty (10^{-15})
HM link to UTC(IT)	0.1
Fountain Dead Time (10%)	0.4
Total (ul/lab)	**0.4**

Table 3. Contributions to ul/lab.

Summary of TAI evaluation results

The final evaluation is obtained using the data reported in Table 2 ($-6.0 \cdot 10^{-15}$), corrected for the final correction value reported in Table 1 ($+43.3 \cdot 10^{-15}$).

MJD Period	y(HM2- ITCsF1)	uA	uB	ul/lab	uRef
55334-55349	$+37.3 \cdot 10^{-15}$ (*)	$0.4 \cdot 10^{-15}$ (#)	$0.5 \cdot 10^{-15}$	$0.4 \cdot 10^{-15}$ (+)	$0.8 \cdot 10^{-15}$ (§)

Table 4. Final results of IT-CsF1 evaluation.

(*) HM2 has the BIPM code 1401103
(#) Including collisional shift evaluation uncertainty (Type A contribution)
(+) Including contribution of uncertainties due to the local link to UTC(IT) and to the fountain dead time.
(§) F. Levi, L. Lorini, D. Calonico, A. Godone “IEN-CsF1 primary frequency standard at INRIM: accuracy evaluation and TAI calibrations” Metrologia 43 No 6 (2006) 545-555

References

[1] F. Levi, L. Lorini, D. Calonico, A. Godone, "IEN-CsF1 accuracy evaluation and Two-Way frequency comparison". IEEE Transactions on Ultrasonics, Ferroelectrics, and Frequency Control, vol. 51, no. 10, pp. 1216-1224 (2004)

[2] F. Levi, L. Lorini, D. Calonico, A. Godone "IEN-CsF1 primary frequency standard at INRIM: accuracy evaluation and TAI calibrations" Metrologia 43 No 6 (2006) 545-555

[3] F. Levi, D. Calonico, L. Lorini, S. Micalizio, A. Godone: "Measurement of the blackbody radiation shift of the ^{133}Cs hyperfine transition in an atomic fountain". Phys. Rev. A, Vol. 70, p. 033412 (2004).

[4] E. Simon, P. Laurent and A. Clairon, "Measurement of the Stark shift of the Cs hyperfine splitting in an atomic fountain" Phys. Rev. A 57, 436 (1998).

[5] S. Micalizio, A. Godone, D. Calonico, F. Levi, L. Lorini: "Blackbody radiation shift of the ^{133}Cs hyperfine transition frequency". Phys. Rev. A, Vol. 69, p. 053401, (2004).

[6] D. Calonico, A. Cina, I. H. Bendea, F. Levi, L. Lorini, and A. Godone "Gravitational red-shift at INRIM, Italy". Metrologia 44, L44-L48, (2007).

[7] J. Vanier and C. Audoin, "The Quantum Physics of Atomic Frequency Standards". Bristol/Philadelphia: Adam Hilger, 1989.

[8] S. R. Jefferts, T. P. Heavner, E. A. Donley and T. E. Parker. "Measurement of Dynamic End-to-End Cavity Phase Shifts in Cesium-Fountain Frequency Standards" IEEE transactions on ultrasonics, ferroelectrics, and frequency control, 51 (2004)

[9] S.R. Jefferts, J.H. Shirley, N. Ashby, E.A. Burt, and G.J. Dick, "Power dependence of distributed cavity phase induced frequency biases in atomic fountain frequency standards" IEEE T. UFFC 52 2314-2321 (2005)
J.H. Shirley, F. Levi, T.P. Heavner, D. Calonico, D.Yu, and S.R. Jefferts, "Microwave Leakage Induced Frequency Shifts in the Primary Frequency Standards NIST-F1 and IEN-CSF1". IEEE T. UFFC 53 2376-2385 (2006)

[10] A. Bauch, J. Achkar, S. Bize, D. Calonico, R. Dach, R. Hlavac, L. Lorini, T. Parker, G. Petit, D. Piester, K. Szymaniec and P. Uhrich, "Comparison between frequency standards in Europe and the USA at the 10^{-15} uncertainty level". Metrologia 43 No 1 (February 2006) 109-120

[11] Dai-Hyuk Yu, Marc Weiss and Thomas E Parker, "Uncertainty of a frequency comparison with distributed dead time and measurement interval offset" Metrologia 44, 91-96 (2007)

[12] G. Panfilo, T. Parker, Proc. 2007 Joint Mtg. IEEE Intl. Freq. Cont. Symp. and EFTF Conf., 805-810, 2007
T. Parker, G. Panfilo, Proc. 2007 Joint Mtg. IEEE Intl. Freq. Cont. Symp. and EFTF Conf., 986-991, 2007

[13] D Calonico, F Levi, L Lorini and G Mana "Bayesian estimate of the zero-density frequency of a Cs fountain", Metrologia 46, 629-636 (2009)

[14] D Calonico, F Levi, L Lorini and G Mana "Bayesian inference of a negative quantity from positive measurement results", Metrologia 46, 267–71 (2009)